Analog stochastic quantization for a one-dimensional binary alloy

N. G. Stocks* and C. J. Lambert

School of Physics and Materials, Lancaster University, Lancaster, LA1 4YB, United Kingdom

R. Mannella

Dipartimento di Fisica, Università di Pisa, Piazza Torricelli 2, 56100 Pisa, Italy

P. V. E. McClintock

School of Physics and Materials, Lancaster University, Lancaster, LA1 4YB, United Kingdom

The technique of analog stochastic quantization (ASQ), originally introduced in relation to the quantum harmonic oscillator, is applied to a more complicated quantum system: namely, a one-dimensional binary alloy. The results from an electronic analog simulator are compared with those obtained from numerical solutions of the Schrödinger equation, with which they are shown to be in agreement. It is argued on this basis that the ASQ technique can in principle be applied to one-dimensional quantum systems with arbitrary potentials.

I. INTRODUCTION

Electronic analog simulation is a well-established tool for finding solutions of awkward nonlinear equations. Although largely eclipsed by digital techniques in relation to deterministic systems (e.g., deterministic chaos[1]), it has enjoyed a resurgence of popularity over the last decade for the treatment of intractable problems in stochastic nonlinear dynamics where exact analytic solutions are frequently unobtainable. Recently a variant of the technique, analog stochastic quantization (ASQ), has been applied[2] successfully to one of the simplest of all quantum mechanical systems—the quantum harmonic oscillator—through exploitation of the well-known mathematical connection[3] that exists between the Schrödinger and Fokker-Planck equations. In the present paper we show how this idea may be extended to the treatment of a rather more complicated quantum system, namely, a one-dimensional (1D) binary alloy. First, however, by way of general background, we review briefly the basis of the analog technique and its role and value in classical stochastic nonlinear dynamics.

The use of electrical circuits to study stochastic nonlinear equations (e.g., Langevin equations), employed by Landauer[4] and Stratonovich,[5] was subsequently extended and developed by a number of other workers including, particularly, Morton and Corrsin.[6] The basis of the technique has been reviewed in detail elsewhere[7] but is, in essence, extremely simple. An electronic circuit is built to model the equation (or system of coupled equations) under study. With use of modern analog components, this procedure is relatively straightforward and can usually be effected in a few hours at most. The various mathematical elements of the equation (e.g., addition, subtraction, integration) can be provided by suitably connected[8] operational amplifiers, or by use of more specialized integrated circuits where appropriate [e.g., the AD 534 (Ref. 9) or MPY 534 (Ref. 10) for multiplication or division, or the AD 639 (Ref. 9) for trigonometric functions]. The circuit model is then driven, as appropriate for the equation under study, by external noise from one or more noise generators and, in some cases, by deterministic forcings as well. The fluctuating voltage(s) representing its response is (are) digitized, and then analyzed by means of a digital computer to calculate and ensemble-average the statistical quantity being sought (e.g., a one-dimensional or multidimensional stationary or time-evolving probability distribution, a spectral density, a correlation function, a first-passage-time distribution, a return-time distribution, or a prehistory probability distribution).

The analog electronic approach to stochastic problems has enjoyed a number of successes, having been used both to confirm some theoretical predictions, and also to rebut a number of others; it has also led to new discoveries in its own right. A full review would be inappropriate here, but highlights of the last decade would include the following: the first demonstrations of noise-induced phase transitions, in the Stratonovich model[11] and the genetic model[12,13] equations, respectively; the first observation of stochastic postponements of critical onsets[14] in a bistable system; measurements of stochastic phase portraits[15] for the double-well Duffing oscillator, leading to the quite unexpected discovery that these become skewed with increasing correlation time of colored noise; the observation of a similar skewing effect in the ring-laser gyroscope equation;[16] investigations of swept parameter systems related to chiral symmetry breaking in prebiotic evolution,[17] transient optical bimodality,[18] the postponement of Hopf bifurcations in the Brusselator,[19] and studies of the role of fluctuations[20] in the laser start-up problem; the first convincing demonstrations of stochastic resonance[21] (SR) and of its occurrence[22] in underdamped systems; a vindication[23] of the proposal that SR be treated in terms of linear response theory and the fluctuation dissipation theorem, a demonstration[24] of the relevance of SR to

sensory neurons, and a resolution[25] of the recent controversy about phase shifts in SR; the rebuttal[26] of a theoretical prediction[27] of a noise-induced divergence in the relaxation time of the Verhulst model; the discovery of modulation-induced negative differential resistance[28] (a deterministic phenomenon); the first observation of supernarrow spectral peaks[29] near a kinetic phase transition; pioneering experiments with quasimonochromatic noise;[30] studies of fluctuation phenomena[31] associated with a multibranch potential; and a demonstration of the physical reality of optimal paths,[32] leading to the unexpected discovery of marked dispersion in the width of the prehistory probability distribution at intermediate time.

In a significant minority of these investigations, digital simulation[33] of the stochastic equations was also used. The question arises, therefore, as to what may be the relative merits of the analog and digital techniques. Although no precise, universally applicable, answer can be given to this question—because their relative advantages and disadvantages naturally depend on the nature of the particular system under study—we can nonetheless offer the following general remarks. First, digital simulation is in general the more accurate of the two approaches provided, of course, that the relevant algorithm has been correctly designed and programmed. Digital simulations are not subject to the parameter drifts, or the effects of internal noise in active components, which can sometimes plague the analog approach. Second, however, for many types of system (especially, but not exclusively, those involving coupled equations, or the combined effects of more than one noise source), digital simulations can become very greedy (often requiring hours) of central processor unit (CPU) time, if the results are to be of reasonable statistical quality. Analog simulations, on the other hand, can produce results of excellent statistical quality relatively quickly (in minutes) to an accuracy typically of a few percent. Third, partly on account of its relative speed, analog simulation readily enables large volumes of parameter space to be surveyed for interesting phenomena, often by turning knobs to adjust the relevant parameters while examining changes in the resultant distribution of a visual display; the equivalent procedure for a digital simulation is usually much slower and more ponderous.

In view of the above considerations, most scientists experienced in both analog and digital simulation seem to regard them as *complementary* techniques for the study of stochastic nonlinear problems. Each of them has its own particular advantages and disadvantages; which of these is emphasized or deemphasized will depend on the properties of the particular equation under study. As in any experimental investigation, it is possible to make mistakes and generate artifacts in either form of simulation. Consequently, in tackling really awkward problems for which there is no existing theory, or where the theory appears to be suspect, it is prudent to use both the analog and the digital simulation techniques together, with the one acting as a check on the other.

Given that electronic analog simulation is of proven value[11−26,28−32] for the investigation of classical systems, it is natural to wonder whether it may also be useful in relation to quantum systems. There is, however, no unique way of applying the technique to a quantum system. One approach would be to try to model the Schrödinger equation directly, treating the real and imaginary parts separately (as was successfully achieved previously[34] in modeling optical bistability under the influence of colored noise). A quite different approach is the ASQ one mentioned above, where we make use of the close correspondence between the Schrödinger and Langevin–Fokker-Planck equations. It is the latter variant of the analog technique that we explore in the present paper, where we treat a quantum system that is significantly more complicated than the one for which ASQ was originally introduced.[2]

ASQ represents a variant of the more conventional stochastic quantization technique,[35,36] adapted for implementation using standard methods[7] of analog electronic simulation. As described in detail elsewhere,[37] stochastic quantization allows information about a quantum mechanical system, such as eigenvalues, eigenfunction intensities, and the density of states, to be obtained by the simulation of a stochastic differential equation (SDE). The SDE is chosen in such a way that its corresponding Fokker-Planck equation reduces to the quantum mechanical eigenvalue problem of interest, but in imaginary time. In the original demonstration[2] of the feasibility of ASQ, applying the technique to the quantum harmonic oscillator it was shown that the eigenvalues and eigenfunction intensities of the lowest-lying excited states could be obtained and that, for higher energies, the density of states could be found from measurements of the partition function. However, the quantum harmonic oscillator is of course a very simple system with a simple analytic (quadratic) potential. In practice one would really like to be able to extend the ASQ technique to facilitate the simulation of a quantum mechanical system with an *arbitrary* potential function.

To this end, we here report the successful simulation of a system with a periodic potential. The potential function (actually the force) was programmed into a bank of EPROM's which were incorporated into a conventionally designed analog simulator. In principle, any potential function can be programmed in this way and, consequently, any one-dimensional (1D) quantum mechanical system can be simulated. The periodic quantum mechanical potential studied here, used to illustrate the technique, consists of alternating negative and positive δ functions and is therefore a simple model of a 1D binary alloy.

II. THEORY
OF ANALOG STOCHASTIC QUANTIZATION

In its simplest form, for a single degree of freedom, x, the ASQ technique starts from a SDE of the Langevin type,

$$\dot{x} = -\frac{\partial W}{\partial x} + \eta(t) , \tag{1}$$

with

$$\langle \eta(t)\eta(t') \rangle = 2D\delta(t - t') ,$$

which has an associated Fokker-Planck equation[37]

$$\frac{\partial \rho(x,t)}{\partial t} = \left[\frac{\partial}{\partial x}\frac{\partial W}{\partial x} + D\frac{\partial^2}{\partial x^2} \right] \rho(x,t) \ . \tag{2}$$

Making the substitution $\rho(x,t) \sim \rho_{\mathrm{eq}}^{1/2}\psi(x,t)$, where $\rho_{\mathrm{eq}}^{1/2} \sim e^{-W/D}$ is the stationary probability density, reduces (2) to an imaginary-time Schrödinger equation of the form

$$-\frac{\partial \psi}{\partial t} = H\psi \ , \tag{3}$$

where

$$H = -D\frac{\partial^2}{\partial x^2} + V(x) \tag{4}$$

and the quantum mechanical potential $V(x)$ is related to $W(x)$ by the Ricatti equation

$$V = \frac{1}{4D}\left[\frac{\partial W}{\partial x}\right]^2 - \frac{1}{2}\frac{\partial^2 W}{\partial x^2} \ . \tag{5}$$

One can now readily show[6] that if $x = x_0$ at $t = 0$, the solution of (2) takes the form

$$\rho(x,t|x_0) = \psi_0(x)\sum_{m=0}^{\infty}\frac{\psi_m(x_0)\psi_m(x)}{\psi_0(x_0)}e^{-\lambda_m t} \ , \tag{6}$$

where $\psi_m(x)$ is an eigenstate of H with eigenvalue λ_m. Thus, by simulating the SDE (1) and measuring $\rho(x,t|x_0)$, information about the quantum mechanical system can be obtained. In practice the return time density $\rho(x,t|x)$, which from (6) is seen to be

$$\rho(x,t|x) = \sum_m \psi_m^2(x)e^{-\lambda_m t} \ , \tag{7}$$

is measured experimentally[2] for an analog electronic circuit model of (1). To obtain estimates of the eigenvalues, Eq. (7) is integrated over x to yield the partition function

$$Z(t) = \sum_{m=0}^{\infty} e^{-\lambda_m t} \ . \tag{8}$$

As long as the eigenvalues are well separated, analysis of (8) at large times gives estimates of the lower-lying eigenvalues. Once these have been obtained, their corresponding eigenfunction intensities ψ_m^2 can be found using (7),

$$\psi_1^2 \sim [\rho(x,t|x) - \psi_0^2]e^{\lambda_1 t} \ .$$

In principle this subtraction of lower-lying eigenstates can be carried on indefinitely, but in practice the cumulative buildup of errors limits the technique to the first two or three levels only.

Finally, one notes that if t is much less than the inverse level separation, (8) can be replaced by an integral to yield

$$Z(t) = \int d\lambda\, N(\lambda)e^{-\lambda t} \ , \tag{9}$$

where $N(\lambda)$ is the density of states at λ. If $N(\lambda)$ varies like λ^P, then this yields, for small t,

$$Z(t) \sim t^{-(P+1)} \ . \tag{10}$$

Therefore the exponent can be extracted from a log-log plot of $Z(t)$ versus t at short t.

Having demonstrated the feasibility[2] of ASQ for the simplest of quantum mechanical systems, namely, the quantum harmonic oscillator, we now show how the method can be modified to facilitate the simulation of an arbitrary 1D potential. For this study the classical Langevin potential $W(x)$ was chosen to be a periodic function with five cells of half-width a, separated by walls of gradient $|\partial W/\partial x| = \alpha/2$, as shown in Fig. 1. The corresponding quantum potential $V(x)$ has alternating positive and negative δ functions, and thus provides a simple model of a one-dimensional binary alloy.

With appropriate boundary conditions we have the Hamiltonian

$$H = \tfrac{1}{4} - \partial_{yy}^2 + \sum_n \delta[y - A(2n+1)] - \delta[y - 2An] \ , \tag{11}$$

where we have defined

$$\beta = \frac{\alpha}{2D}, \quad A = \beta a \ , \tag{12}$$
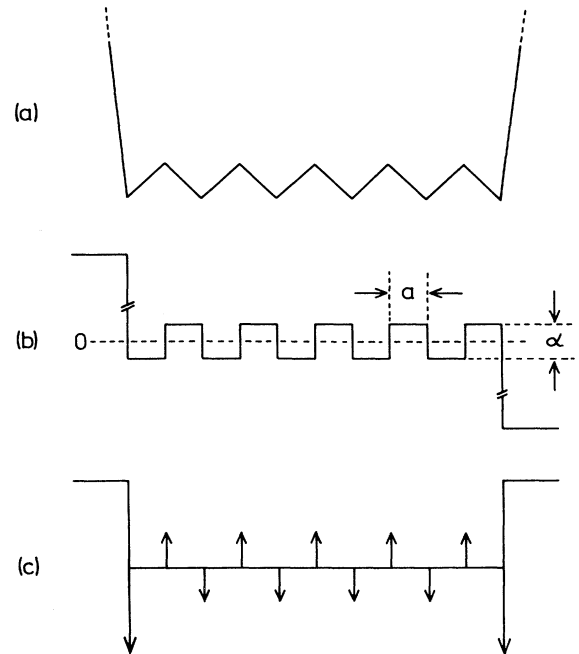
and the dimensionless variables

FIG. 1. (a) Classical potential $W(x)$ used in the Langevin equation (1) in order to simulate a quantum mechanical one-dimensional alloy. It is periodic, with five cells of half-width a, and with end walls that are finite but very much higher than the cellular potential maxima. (b) The corresponding force $-\partial W(x)/\partial x$ programmed into EPROM's for the digital function generator. There are ten forcing regions of magnitude $|\alpha/2|$ and width a. (c) The corresponding quantum mechanical potential $V(x)$ given by Eq. (5). The arrows represent positive and negative δ functions.

$$y = \beta x, \quad \tau = D\beta^2 t \tag{13}$$

have been introduced. The return density (7) is then given by

$$\rho(y, \tau | y) = \sum_n \psi_n^2(y) e^{-\lambda_n \tau} .$$

III. ANALOG SIMULATION

The electronic analog simulator used to study Eq. (1) was in part of conventional design[7] and is shown schematically in Fig. 2(a). However, an unusual feature of this circuit is the incorporation of a digital function generator (DFG) to generate the forcing function $\partial W / \partial x$. The DFG is similar in general design to one used earlier[16] and is shown schematically in Fig. 2(b). It consists of an analog-to-digital converter (ADC), which transforms the analog signal $x(t)$ into a 12-bit address which is then used to access one of the 4K memory locations in the EPROM's, where the forcing function had previously been programmed. Therefore, the forcing function could be specified at any given $x(t)$. Finally, a digital-to-analog converter (DAC) was used to convert the digitally encoded force back into an analog voltage. The processing time of the DFG, which introduced a slight delay in the system, was 4 μs. The circuit was therefore time scaled so as to ensure that this was by far the shortest time scale in the system. For all the results reported $D = 0.10, \beta = 5$, and $A = 4.2$.

The data processing was carried out by a Nicolet 1180 data processor. The processor discretized $x(t)$ in both x and t, with a 12-bit precision in x and 256 or more time channels. The sampling interval was set either to 10 or 8000 μs, which reflects the differing time scales of interest (energies of interest) in the eigenvalue spectrum. The return density was constructed using the algorithm described previously.[2]
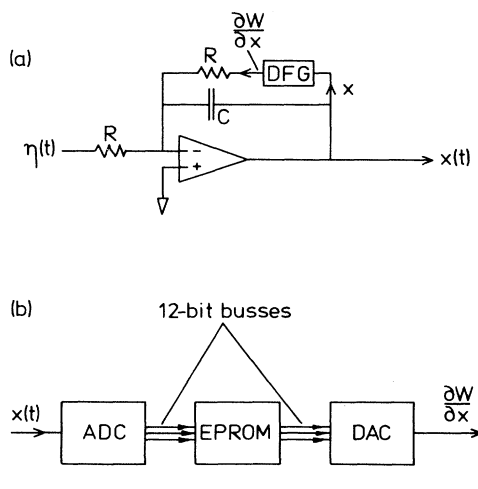
A typical example of a realization of $x(t)$, obtained from the analog simulator is shown in Fig. 3. The "particle" can clearly be seen to be diffusing between the stable states corresponding to the potential minima. Two return densities measured for different time scales are shown in Figs. 4(a) and 4(b). Because of the periodic nature of the potential, the eigenvalues form in bands of five, there being five unit cells comprising our lattice. The first band, formed by the hybridization of the lowest-lying bound states of isolated cells, is characterized by relatively small eigenvalues $\sim 10^{-3}$. Consequently, a large τ is necessary to allow the excited states of the lowest band to decay, thus enabling the ground-state eigenfunction intensity $\rho(y)$ to be obtained from the relation $\lim_{\tau \to \infty} \rho(y, \tau | y) \to \rho(y)$. Figure 4(a) shows, predominantly, the decay of the first band, the ground state being just about approached at $\tau \sim 2500$, as shown, in Fig. 5(a). Figures 5(b) and 5(c) show other slices obtained from $\rho(y, \tau | y)$ at two different times τ. Although it is in principle possible to obtain estimates for the higher-order eigenfunction intensities, by subtraction of the ground states from slices such as these,[2] this procedure cannot be carried out in the present case. This is due to the banded nature of the eigenvalue spectrum, in which the lower-lying eigenvalues are insufficiently well separated to allow a subtraction to be made unambiguously.

To judge the accuracy of the technique, the eigenvalue problem associated with (1) was also solved numerically by digital computer and the results compared with the data obtained from the analog simulation. The problem can be cast in the form of a free wave scattered by the δ functions, with appropriate boundary conditions. Clearly, the propagation of the Bloch wave from one boundary to the other is given by a product of spatial transfer matrices and δ-function scattering matrices. The eigenvalue spectrum is then computed subject to the requirement that the Bloch wave satisfies the boundary conditions.

FIG. 2. (a) Schematic diagram of the analog electronic circuit used to model the one-dimensional alloy. (b) The digital function generator (DFG).
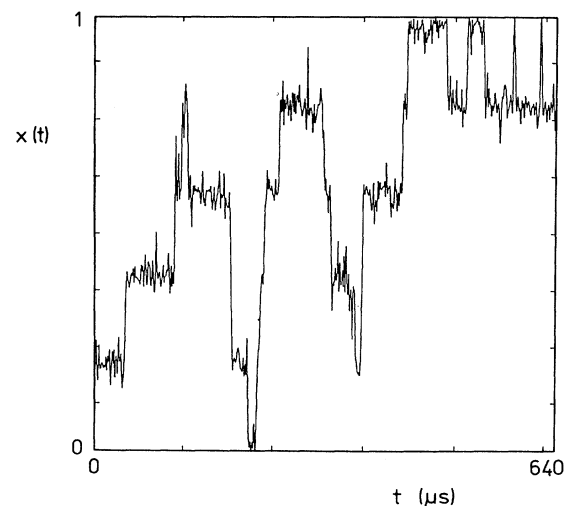

FIG. 3. Typical $x(t)$ trajectory for the electronic circuit model of the one-dimensional alloy, showing temporary residence in each of the (classical) potential wells of Fig. 1(a).

The problem is solved by noting that, in the flat regions between δ functions, any eigenstate of H will be of the form

$$\psi(x) = B_+ e^{ikx} + B_- e^{-ikx} \tag{14}$$

and the plane-wave amplitudes $B_\pm$ of the cell to the left of a δ function of strength Δ are related to the amplitudes $B'_\pm$ of the cell to the right by

$$\begin{bmatrix} B_+ \\ B_- \end{bmatrix} = T \begin{bmatrix} B'_+ \\ B'_- \end{bmatrix}, \tag{15}$$

where

$$T = \begin{vmatrix} 1 + \dfrac{\Delta}{2ik} & \dfrac{\Delta}{2ik} e^{-2ikx_0} \\ -\dfrac{\Delta}{2ik} e^{2ikx_0} & 1 - \dfrac{\Delta}{2ik} \end{vmatrix}.$$

The boundary conditions need special care. In fact, for the region outside the 1D alloy, as well as two negative δ functions located at the boundary, the actual potential $W(x)$ used in the analog simulations gives a quantum mechanical potential which is large but finite. From the Riccati equation, if the negative δ functions at the boundaries are of strength $-(D + \frac{1}{2})$, where D is a large quan-
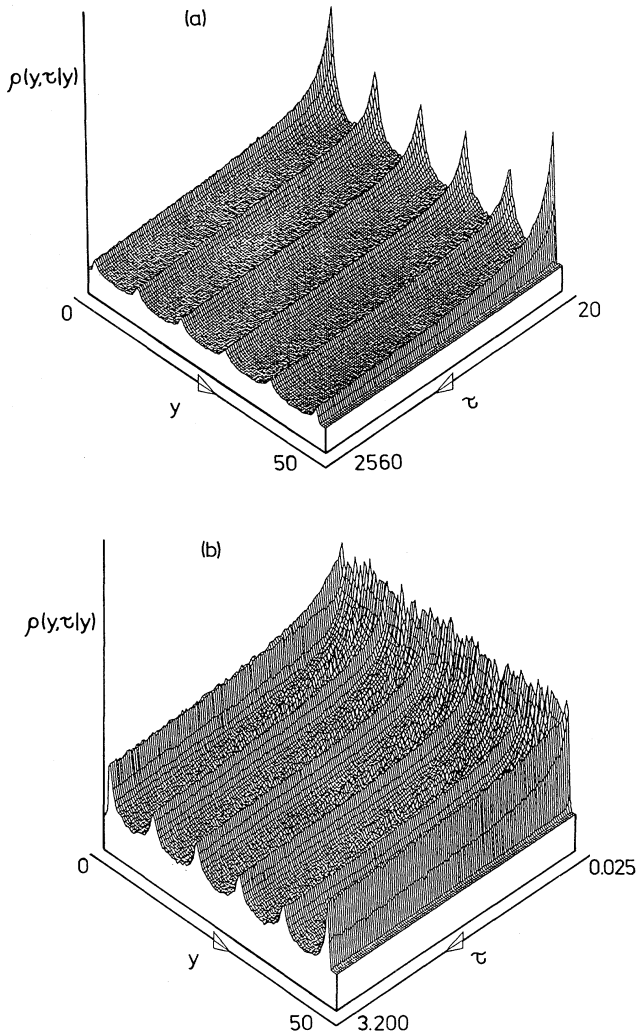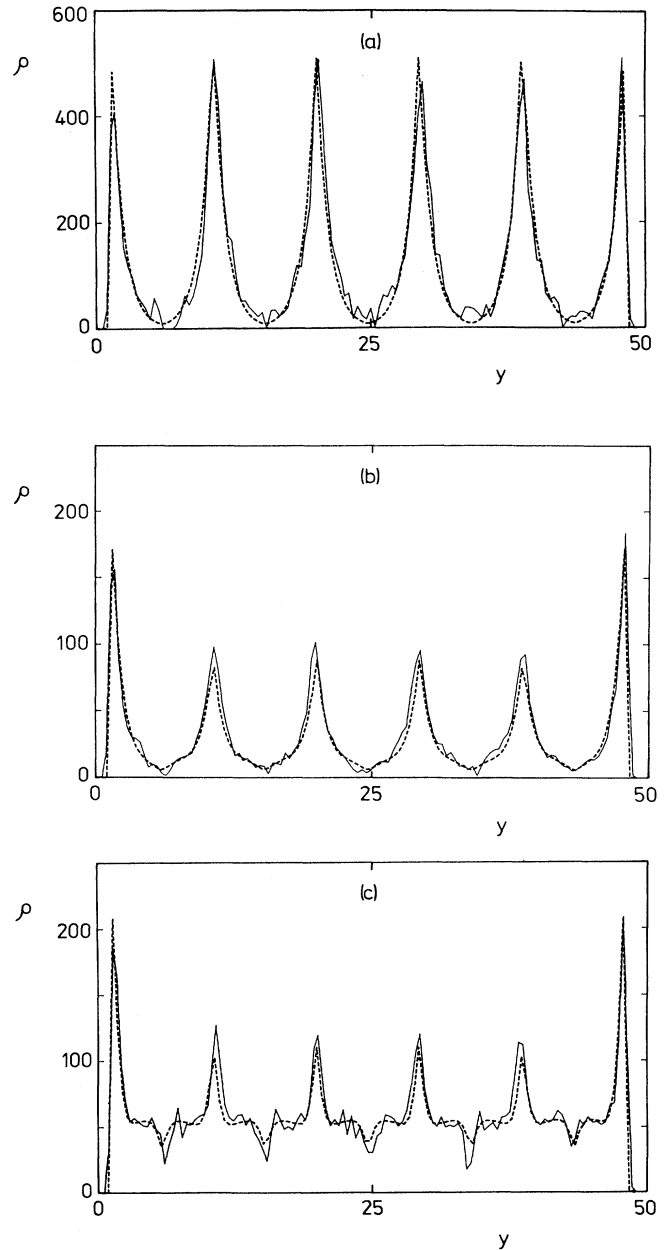

FIG. 4. Return-time probability densities $\rho(y,\tau|y)$ measured for the electronic circuit model: (a) over long times and (b) over shorter times.

FIG. 5. Sections through return-time probability densities $\rho(y,\tau|y)$ measured in counts (solid curves) for the electronic simulator: (a) at $\tau=2560$, (b) at $\tau=3.2$, and (c) at $\tau=0.8$. The dashed curves represent numerical computations for the quantum mechanical system, scaled vertically to match the experiment.

tity, we find that the potential in the classically inaccessible region is given by $D^2 - \frac{1}{4}$, where we have assumed that the potential in the accessible region has the value zero. It is straightforward to modify the theory to account for these peculiarities. As expected, we find that the vector k becomes imaginary in the classically forbidden region, and we require on physical grounds that the amplitude of the exponentially increasing function vanishes. For a boundary located at x_0, the plane-wave amplitudes $B_\pm$ of the adjacent cell, taking into account both the finite height of the potential and the negative δ function, are given by

$$B_+ = \frac{B_0}{2} \left[1 \pm \frac{\chi - (D + \frac{1}{2})}{ik} e^{x_0(\chi - ik)} \right] , \qquad (16)$$

$$B_- = \frac{B_0}{2} \left[1 \mp \frac{\chi - (D + \frac{1}{2})}{ik} e^{x_0(\chi + ik)} \right] , \qquad (17)$$

where B_0, the amplitude of the wave function in the forbidden region, is <u>determined from</u> normalization conditions and $\chi = \pm \sqrt{D^2 - 1/4 - k^2}$. The upper (lower) sign

of χ corresponds to the left (right) boundary.

To compute the allowed k vectors [and hence the allowed eigenvalues and wave functions $\psi(x)$], we choose a trial k and set $B_0 = 1$ in the classically inaccessible region to the left. The wave function in the classically forbidden region to the right is then obtained from a product of transfer matrices and the allowed values of k obtained from the condition that the wave function in this region must decay for large x.

In practice, Bloch wave functions with boundary conditions corresponding to an infinite potential barrier plus an infinite negative δ function are close enough to the exact solution to give a good initial guess for the allowed k vectors, at least for the lowest eigenvalues.

IV. DISCUSSION

The experimental $\rho(y, \tau | y)$ cross sections (solid curves) from the analog simulation are compared with the numerically computed ones (dashed curves) in Figs. 5(a)–5(c). The agreement is clearly very good, especially if some allowance is made for the discretization (128
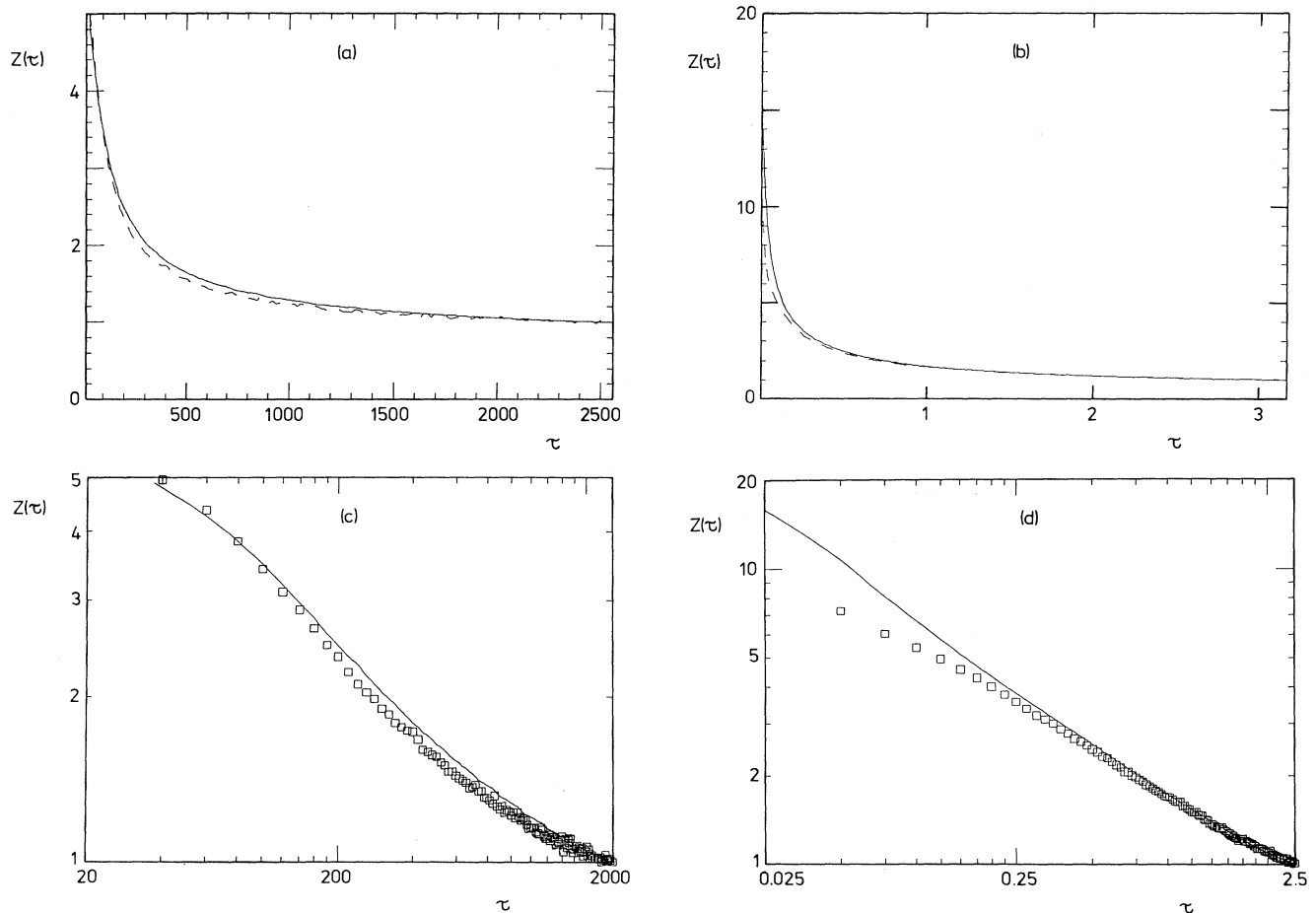

FIG. 6. Partition function $Z(\tau)$ for the one-dimensional alloy (arbitrary ordinate units); Measurements made with the electronic simulator (dashed lines or squares) are compared with numerical computations (solid curves): (a) for large times, (b) for short times, (c) for large times on a double logarithmic scale, and (d) for short times on a double logarithmic scale.

values) of the abscissa in the experimental case, which has the effect of reducing the height of sharp peaks. The characteristic changes of shape with τ found in the experiment are also seen to occur in the calculated curves. In Fig. 6(a) and 6(b) the numerically computed partition function $Z(\tau)$ is compared with that obtained from the analog simulation. It can be seen that, as in the case of the cross sections, the agreement between the two curves is good, thus confirming that the analog circuit accurately simulates the quantum mechanical system. The logarithm of the partition function is shown in Figs. 6(b) and 6(c). Again the theory is seen to describe the experimental data well. This discrepancy which is observed at small τ is due to the truncation of the summation in (8). At such large energies (small τ) very few of the eigenstates have decayed and thus an excessively large number of terms would be needed to obtain an accurate result.

One interesting feature of the small τ data [Fig. 6(d)] is that the gradient at $\tau \sim 2$ is $\sim -\frac{1}{2}$. This reflects [see Eq. (10)] the fact that, at this value of energy, the quantum system approaches that of the free-electron model, with its well known $E^{-1/2}$ density of states. At still smaller τ (larger energies) the gradient is seen to decrease; this is due to the finite barrier height of the boundaries in the quantum mechanical system.

We note that any potential function $W(x)$ could have been inserted in the EPROM's of the DFG: It is not necessary that $W(x)$ should be of a simple analytic form. The above results therefore demonstrate that the ASQ technique may be extended to allow the simulation of an *arbitrary*, time-independent, one-dimensional quantum system. However, they have also highlighted an inherent limitation of the technique in relation to systems whose low-lying eigenvalues are close together, in that it then becomes impossible in practice to extract the lower eigenvalues or eigenfunction intensities unambiguously using (7) and (8). The latter method worked well[2] for the quantum harmonic oscillator precisely because its eigenvalues are well separated, whereas the one-dimensional alloy considered here represents an example of a system for which the procedure cannot be used. For the future, it will be of interest to determine whether such problems can be circumvented by direct electronic simulation of the full, real-time, Schrödinger equation. Such investigations are currently in progress.

ACKNOWLEDGMENTS

*Present address: Department of Engineering, University of Warwick, Coventry, CV4 7AL, United Kingdom.
[1]J. M. T. Thompson and H. B. Stewart, *Nonlinear Dynamics and Chaos* (Wiley, New York, 1986).
[2]N. G. Stocks, C. J. Lambert, and P. V. E. McClintock, J. Stat. Phys. **54**, 1397 (1988).
[3]H. Risken and H. D. Vollmer, Z. Phys. **204**, 240 (1967).
[4]R. Landauer, J. Appl. Phys. **33**, 2209 (1962).
[5]R. L. Stratonovich, *Topics in the Theory of Random Noise* (Gordon and Breach, New York, 1967), Vols. I and II.
[6]J. B. Morton and S. Corrsin, J. Math. Phys. **10**, 361 (1969).
[7]L. Fronzoni, in *Noise in Nonlinear Dynamical Systems,* edited by F. Moss and P. V. E. McClintock (Cambridge University Press, England, 1989), Vol. 3, p. 222; P. V. E. McClintock and F. Moss, in *ibid.*, p. 243.
[8]P. Horowitz and W. Hill, *The Art of Electronics* (Cambridge University Press, Cambridge, England, 1980).
[9]Analog Devices Inc., Box 9106, Norwood, MA 02062.
[10]Burr-Brown Inc., Box 11400, Tucson, AZ 85734.
[11]J. M. Sancho, M. San Miguel, H. Yamazaki, and T. Kawakubo, Physica **116A**, 560 (1982).
[12]J. Smythe, F. Moss, and P. V. E. McClintock, Phys. Rev. Lett. **51**, 1062 (1983).
[13]J. Smythe, F. Moss, P. V. E. McClintock, and D. Clarkson, Phys. Lett. **97A**, 95 (1983).
[14]S. D. Robinson, F. Moss, and P. V. E. McClintock, J. Phys. A **18**, L89, (1985); P. V. E. McClintock and F. Moss, Phys. Lett. **107A**, 367 (1985).
[15]F. Moss, P. Hänggi, R. Mannella, and P. V. E. McClintock, Phys. Rev. A **33**, 4459 (1986).
[16]K. Vogel, H. Risken, W. Schleich, M. James, F. Moss, R. Mannella, and P. V. E. McClintock, Phys. Rev. A **35**, 463

(1987); J. Appl. Phys. **62**, 721 (1987).
[17]D. K. Kondepudi, F. Moss, and P. V. E. McClintock, Physica **21D**, 296 (1986).
[18]W. Lange, in *Noise in Nonlinear Dynamical Systems* (Ref. 7), Vol. 3, p. 159, and references therein.
[19]L. Fronzoni, R. Mannella, P. V. E. McClintock, and F. Moss, Phys. Rev. A **36**, 834 (1987).
[20]J. Casademunt, J. I. Jimenez-Aquino, J. M. Sancho, C. J. Lambert, R. Mannella, P. Martano, P. V. E. McClintock, and N. G. Stocks, Phys. Rev. A **40**, 5915 (1989); N. G. Stocks, R. Mannella, and P. V. E. McClintock, *ibid.* **40**, 5361 (1989); **42**, 3356 (1990).
[21]S. Fauve and F. Heslot, Phys. Lett. **97A**, 5 (1983).
[22]L. Gammaitoni, F. Marchesoni, E. Menichella-Saetta, and S. Santucci, Phys. Rev. Lett. **62**, 349 (1989).
[23]M. I. Dykman, R. Mannella, P. V. E. McClintock, and N. G. Stocks, Phys. Rev. Lett. **65**, 2606 (1990).
[24]A. Longtin, A. Bulsara, and F. Moss, Phys. Rev. Lett. **67**, 656 (1991).
[25]M. I. Dykman, R. Mannella, P. V. E. McClintock, and N. G. Stocks, Phys. Rev. Lett. **68**, 2985 (1992).
[26]P. J. Jackson, C. J. Lambert, R. Mannelia, P. Martano, P. V. E. McClintock, and N. G. Stocks, Phys. Rev. A **40**, 2875 (1989).
[27]H. K. Leung, Phys. Rev. A **37**, 1341 (1988).
[28]R. C. M. Dow, C. J. Lambert, R. Mannella, and P. V. E. McClintock, Phys. Rev. Lett. **59**, 6 (1987).
[29]M. I. Dykman, R. Mannella, P. V. E. McClintock, and N. G. Stocks, Phys. Rev. Lett. **65**, 48 (1990).
[30]M. I. Dykman, P. V. E. McClintock, N. D. Stein, and N. G. Stocks, Phys. Rev. Lett. **67**, 933 (1991).
[31]M. I. Dykman, D. G. Luchinsky, P. V. E. McClintock, N. D.

Stein, and N. G. Stocks, Phys. Rev. A **45**, R7678 (1992).

[32]M. I. Dykman, P. V. E. McClintock, V. N. Smelyanski, N. D. Stein, and N. G. Stocks, Phys. Rev. Lett. **68**, 2718 (1992).

[33]R. Mannella, in *Noise in Nonlinear Dynamical Systems* (Ref. 7), p. 189, and references therein.

[34]P. Grigolini, L. A. Lugiato, R. Mannella, P. V. E. McClintock, M. Merri, and M. Pernigo, Phys. Rev. A **38**, 1966

(1988).

[35]S. Duane and J. B. Kogut, Nucl. Phys. **B275**, 398 (1986).

[36]S. Duane, A. D. Kennedy, B. J. Pendleton, and D. Roweth, Phys. Lett. B **195**, 216 (1987).

[37]T. Schneider, M. Zannetti, and R. Badii, Phys. Rev. B **31**, 2941 (1985); H. Risken, *The Fokker-Planck Equation* (Springer, Berlin, 1984).